Biocatalysis and Biotransformation

ISSN: (Print) (Online) Journal homepage: https://www.tandfonline.com/loi/ibab20

Biotransformation of pungent constituents from ginger (*Zingiber officinale* Roscoe) by *Colletotrichum gloeosporioides* yields oxidative *ortho–ortho* coupling products

Roberta Marques Dias de Ávila, Leonardo Toffano, João Batista Fernandes, Maria Fátima das Graças Fernandes da Silva, Lorena Ramos Freitas de Sousa & Paulo Cezar Vieira

To cite this article: Roberta Marques Dias de Ávila, Leonardo Toffano, João Batista Fernandes, Maria Fátima das Graças Fernandes da Silva, Lorena Ramos Freitas de Sousa & Paulo Cezar Vieira (2021): Biotransformation of pungent constituents from ginger (*Zingiber officinale* Roscoe) by *Colletotrichum gloeosporioides* yields oxidative *ortho–ortho* coupling products, Biocatalysis and Biotransformation, DOI: 10.1080/10242422.2021.1878159

To link to this article: https://doi.org/10.1080/10242422.2021.1878159

BIOCATALYSIS AND BIOTRANSFORMATION
https://doi.org/10.1080/10242422.2021.1878159

Taylor & Francis
Taylor & Francis Group

REAEARCH ARTICLE

Biotransformation of pungent constituents from ginger (*Zingiber officinale* Roscoe) by *Colletotrichum gloeosporioides* yields oxidative *ortho–ortho* coupling products

Roberta Marques Dias de Ávila[a], Leonardo Toffano[b], João Batista Fernandes[a], Maria Fátima das Graças Fernandes da Silva[a], Lorena Ramos Freitas de Sousa[c] and Paulo Cezar Vieira[a,d]

[a]Department of Chemistry, Federal University of São Carlos, São Paulo, Brazil; [b]Department of Agronomy, Brasil University, Descalvado, Brazil; [c]Special Academic Unit of Chemistry, Federal University of Goiás, Catalão, Brazil; [d]School of Pharmaceutical Sciences of Ribeirão Preto, University of São Paulo, Ribeirão Preto, Brazil

ABSTRACT

This work investigated the biotransformation of ginger constituents (zingerone, [6]-shogaol, [6]-gingerol, and methyl-[6]-gingerol) by the pathogenic fungus *Colletotrichum gloeosporioides*. Experiments were carried out with and without deuterium-labelled compounds. The product metabolites were analyzed by liquid chromatography coupled to tandem mass spectrometry and liquid chromatography solid phase extraction-nuclear magnetic resonance. Substrates supplied to the fungus were incorporated into metabolic pathways mostly by oxidation reactions, including aromatic carbon–carbon coupling. Zingerone and [6]-gingerol biotransformation products included biphenol dimers. A biodegradation pathway for biphenol formation was proposed based on the presence of the intermediate 4-(2-hydroxyethyl)-2-methoxyphenol, commonly identified from [6]-gingerol and [6]-shogaol biodegradation. This intermediate likely originates from a Baeyer–Villiger reaction followed by hydrolysis. The C–C coupling of molecules could result in phenolic oxidative *ortho–ortho* coupling, suggesting that biphenol dimers are products of *C. gloeosporioides* laccase catalysis.

GRAPHICAL ABSTRACT

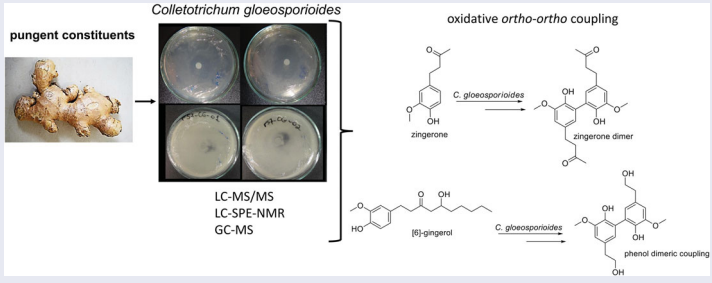

ARTICLE HISTORY
Received 15 June 2020
Revised 6 January 2021
Accepted 13 January 2021

KEYWORDS
Biotransformation; *Colletotrichum gloeosporioides*; biphenol; ginger

Introduction

Zingiber officinale Roscoe (Zingiberaceae family), commonly known as ginger, is a root used worldwide as a food and beverage additive and is also found in traditional medicines for the treatment of several diseases (Kubra and Rao 2012; Baliga et al. 2013; Villalvilla et al. 2014; Bartels et al. 2015; Prasad and Tyagi 2015; Semwal et al. 2015; Azimi et al. 2016; Choi et al. 2018; Kou et al. 2018). Pharmacological properties of ginger include antioxidative, anticancer, antimicrobial, and anti-inflammatory activities (Citronberg et al. 2013; Ho et al. 2013; Mashhadi et al. 2013; Kumar et al. 2014; Nile and Park 2015).

Primary and secondary metabolites have been previously identified from ginger. The pungent constituents have been shown to be the major compounds responsible for the biological activities associated with ginger (Jolad et al. 2004; Mashhadi et al. 2013; Choi et al. 2018). Dehydration of [6], [8], and [10]-gingerols yields the corresponding shogaols from dried ginger (Bhattarai et al. 2007) that, after hydrogenation by

CONTACT Paulo Cezar Vieira pcvieira@fcfrp.usp.br School of Pharmaceutical Sciences of Ribeirão Preto, University of São Paulo, Ribeirão Preto 14040-903, Brazil

Supplemental data for this article can be accessed here.

microorganisms, become paradols (Stoner 2013). [6]-Shogaol, one of the main pungent constituents of ginger, has confirmed biological properties, including antibacterial, anti-hepatotoxic, antioxidative, anti-cancer, and anti-inflammatory activities (Semwal et al. 2015; Jo et al. 2016; Kou et al. 2018). Heating or drying ginger root activates the retro-aldol reaction of gingerol, generating zingerone, another compound with pharmacological potential (Ahmad et al. 2015). Previously, we investigated the chemical and biological properties of ginger metabolites, and we found that [10]-gingerol is a promising compound for the treatment of triple negative breast cancer (Martin et al. 2017; Fuzer et al. 2019).

Chemical modification of the phenolic compounds from ginger could improve their pharmacological properties and potential therapeutic applications. Organic synthesis is challenging, but the microorganisms or their enzymatic systems may be powerful tools for accomplishing desired chemical transformations (García-Pajón et al. 2003). The biotransformation of [6]-shogaol by *Aspergillus niger* (Takahashi et al. 1993; Lee 1995; Lee and Lee 1995; Jo et al. 2016) and *Schizosaccharomyces pombe* (Choi et al. 2017) produced new lead compounds, such as [6]-paradol, which had significant pharmacological activities and higher bioavailability than [6]-shogaol (Jo et al. 2016; Choi et al. 2017).

In this work, we increased the chemical diversity of ginger metabolites by using the pathogenic fungus *Colletotrichum gloeosporioides* to transform ginger constituents (zingerone, [6]-shogaol, [6]-gingerol, and methyl-[6]-gingerol). *Colletotrichum gloeosporioides* is capable of oxidoreductase activity, promoting regioselective hydroxylations and diastereo- and enantioselective reductions on different substrates (Miyazawa et al. 1995; Miyazawa and Wada 2000; García-Pajón et al. 2003). To investigate the fungal biotransformation of ginger metabolites, compounds with and without deuterium labelling were prepared as substrates for *C. gloeosporioides*, and fungal metabolites were analyzed using GC-MS, LC-MS/MS, and LC-SPE-NMR.

Materials and methods

General materials

The fungus *C. gloeosporioides* (Penz.) Penz. & Sacc. was furnished by the Laboratory of Physiology and Phytopathological Biochemistry, Luiz de Queiroz College of Agriculture, University of São Paulo (USP, Piracicaba, SP, Brazil). Potato dextrose agar (PDA) medium was obtained from Neogen Corporation (Lansing, MI, USA), and zingerone (CAS 122-48-5) and lithium bis(trimethylsilyl)amide solution (CAS 4039-32-1) were purchased from Sigma-Aldrich (St. Louis, MO, USA). Ginger rhizome (6 kg) was purchased locally (São Carlos, SP, Brazil).

[6]-Gingerol was obtained by purification from the fresh ginger rhizome (Da Silva et al. 2012). Methyl-[6]-gingerol and [6]-shogaol were derived from [6]-gingerol reactions (Villalvilla et al. 2014). The deuterium labelling reaction (Tamogami et al. 2016) was performed on [6]-gingerol and zingerone, yielding [6]-gingerol-D_3 (54%) and zingerone-D_5 (66.3%), respectively. Further information about purification procedures, syntheses, and additional materials (^{1}H NMR and MS data) are described in the Supplementary Information.

A Shimadzu SCL-10AVP high-performance liquid chromatography (HPLC) instrument with an LC-6AD photodiode array detector was used for purification (Shimadzu, Columbia, MD, USA). Structural characterization of compounds was completed using nuclear magnetic resonance spectroscopy (NMR), gas chromatography-mass spectrometry (GC-MS), HPLC coupled to a triple quadrupole MS system with electrospray ionization (ESI) (LC-ESI-MS/MS), and liquid chromatography-solid phase extraction-nuclear magnetic resonance (LC-SPE-NMR). The instruments used were: DRX-400 NMR (Bruker, Billerica, MA, USA) with a 9.4 Tesla magnet (^{1}H: 400 MHz; ^{13}C: 100 MHz); GC 2010 Plus and MSTQ8030 (Shimadzu); MDS-Sciex API 2000 LC-ESI-MS/MS (Applied Biosystems, Foster, CA, USA); HPLC (Shimadzu) coupled to an Esquire 6000 ion trap (IT) mass spectrometer (Bruker) (LC-IT-MS/MS); and LC (Agilent, Barueri, SP, Brazil) coupled to an automatic cartridge exchanger Bruker/Spark Prospekt 2 SPE unit (Bruker BioSpin, Rheinstetten, Germany) and a Bruker Daltonik NMR 600 MHz spectrometer with a 14.1 Tesla magnet (LC-SPE-NMR).

Solvents for chromatographic procedures (ethanol, *n*-hexane, ethyl acetate (EtOAc), and methanol (MeOH)) were from Vetec (Duque de Caxias, RJ, Brazil). HPLC grade solvents (MeOH, acetonitrile (ACN), and water) were obtained from Merck (Darmstadt, HE, Germany). Deuterated solvents (chloroform ($CDCl_3$), methanol (CD_3OD), and tetramethylsilane (TMS)) were acquired from and Sigma-Aldrich. Silica gel 60 (SiO_2, 70–230 mesh) and thin-layer chromatography (TLC) on pre-coated aluminium silica 60 F_{254} were from Merck. TLC was used to monitor compounds from chromatography procedures and from synthesis reactions by $UV_{254/366}$ and reaction with sulphuric vanillin solution.

Microorganism pre-inoculation with the substrate

Cultures of *C. gloeosporioides* were maintained on potato dextrose agar (PDA) plates at 25 °C. After

incubation for 7 days, spores and mycelia were suspended in sterile water (2 mL). To evaluate substrate toxicity, experiments in test tubes and enzyme-linked immunosorbent assay (ELISA) 96-well plates were performed. Serial dilutions using a stock solution of 1600 mg mL^{-1} led to concentrations of 0.1–15 mg mL^{-1} in the test tubes. In the ELISA plate experiments, 20 μL of inoculum (spore and mycelium suspension) was mixed with 80 μL of sterile culture medium (PDA) contained fungi culture in each well. Then 100 μL of individual substrates dissolved in sterile water and DMSO (zingerone, [6]-shogaol, [6]-gingerol, and methyl-[6]-gingerol) were added to final concentrations of 0.781–400 μg mL^{-1}. The positive control was the antifungal compound actidione and the negative control was sterile PDA medium without substrate. After incubation of both test tubes and plates for 15 days at 30 °C, toxicity was visually evaluated by observing mycelium growth.

Large-scale biotransformation of zingerone and purification of products

Two *C. gloeosporioides* mycelial plugs (0.5 cm diameter), cut from the growing edge of a PDA plate, were added to 60 mL test tubes containing 15 mL of sterile liquid potato dextrose (PD). After 7 days of fermentation (30 °C, 120 rpm), 1.0 mL of this active mycelium suspension was transferred to 30 mL test tubes containing 8 mL of sterile liquid potato dextrose and 1 mL of zingerone dissolved in sterile water and DMSO (final concentrations: 1.0; 5.0; 10.0; 15.0 mg mL^{-1}). After 15 days of incubation at room temperature, mycelium growth was only observed in tubes containing 1.0 mg mL^{-1} zingerone. The control without substrate (control A) and control without fungal inoculation but with the substrate (control B) were prepared in the same conditions. All controls and experiments were performed in quintuplicate.

After the incubation period, culture media containing mycelia were filtered. The combined filtrate obtained from test tubes with 1.0 mg mL^{-1} of zingerone was extracted with EtOAc (3 × 20 mL), affording extract (A) (9 mg). The tubes with 5–15 mg mL^{-1} of zingerone were combined and extracted with EtOAc (3 × 60 mL), affording extract (B) (960 mg). The solvent from extracts A and B was removed by rotary evaporation under reduced pressure (40 °C). The extract (B) was fractionated on a silica gel 60 column (2.5 × 11 cm; *n*-hexane–EtOAc 7:3 (1000 mL, isocratic)), affording 17 fractions. The fourth fraction (N-4) (4.0 mg) was identified by high-resolution MS and NMR experiments as a zingerone dimer, 4,4′-(6,6′-dihydroxy-5,5′-dimethoxy-[1,1′-biphenyl]-3,3′-diyl) bis (butan-2-one)] (**1**), (Slavova-Kazakova et al. 2015). ESI-MS: $[M + Na]^+$ *m/z* 409.1648, M of *m/z* ($C_{22}H_{26}O_6$, 386.1729 calcd.); ^1H NMR ($CDCl_3$) δ_H ppm 2.16 (*s*, 6H), 2.78 (*d*, 4H), 2.88 (*d*, 4H), 3.92 (*s*, 6H), 6.75 (*d*, $J = 4.0$ Hz, 2H), 6.73 (*d*, $J = 4.0$ Hz, 2H).

Optimized conditions with substrates: zingerone, zingerone-D_5, [6]-gingerol, [6]-gingerol-D_3, methyl-[6]-gingerol and [6]-shogaol

Three *C. gloeosporioides* mycelial plugs (0.5 cm diameter), cut from the growing edge of a PDA plate, were transferred under sterile conditions to Erlenmeyer flasks (250 mL) containing 50 mL of sterile liquid PD. After 48 h of fermentation (30 °C, 120 rpm), 0.5 mL aliquots of substrate solutions (100 μg mL^{-1} in DMSO) were added and the cultures were incubated for 10 days (30 °C, 120 rpm). A control without substrate addition (control A) and control without fungal inoculation (control B) were prepared in the same conditions. All experiments were performed in triplicate.

After the incubation period, the culture media containing mycelia were filtered. The mycelia were extracted with MeOH for 4 days and agitated with an ultrasound probe for 30 min. The filtrate was extracted with EtOAc (3 × 20 mL). Solvent removal by rotary evaporation under reduced pressure (40 °C) yielded an organic extract of EtOAc, a methanolic extract (MM), and an aqueous extract. The extraction process for the controls was performed in the same manner. Fungal metabolites were identified in the EtOAc extracts of samples by LC-MS/MS, LC-SPE-NMR, and GC-MS.

Experiments for metabolite profiling

The EtOAc extract and control A, control B, were diluted in 10% MeOH (1 mg mL^{-1} in water) and filtered (Millipore, 0.20 μm).

For *Methods I*, *II*, and *III*, an Eclipse XDB-C_{18} Phenomenex (5 μm particle size; 150 × 4.6 mm) (Agilent) column connected to a C_{18} (5 μm; 4 × 30 mm) (Allcrom, São Paulo, SP, Brazil) was used. The flow rate for all methods was 1.0 mL min^{-1}. Unless otherwise noted, peak detection was monitored at 220 nm.

Method I: The mobile phase was composed of H_2O (A) and ACN or MeOH (B). The method started with a gradient of 10–37% (B) over 3 min, followed by 37% (B) for 7 min (isocratic), a linear gradient of 37–55% (B) over 2 min, a linear gradient of 55–100% (B) over 10 min (%Δ ACN = 4.5), and 100% (B) for 12 min. The

column was cleaned for 20 min using 100% (B), and a conditioning cycle time of 30 min brought the column back to the initial condition (10% (B)).

Method II: The mobile phase was composed of H_2O (A) and MeOH or ACN (B). The method started with 5 min of 10% (B), followed by a linear gradient of 10–100% (B) over 20 min (%Δ MeOH = 4.5), and 20 min of 100% (B). Column cleaning and a conditioning cycle time of 20 min returned the column to the initial condition (10% (B)).

Method III: The mobile phase consisted of H_2O (A) and ACN (B) with 0.1% *v/v* formic acid in both solvents. A linear gradient increasing solvent (B) 10–100% (%Δ MeOH = 4.5), followed by 20 min of 100% (B) was used. Column cleaning and a conditioning cycle time of 20 min returned the column to the initial condition (10% (B)).

LC-ESI-MS/MS

Selected reaction monitoring (SRM) experiments were carried out in positive $[M+H]^+$ and negative $[M-H]^-$ modes using an HPLC (Agilent) coupled to a API2000 spectrometer containing a triple quadrupole and an electrospray ionization source (ESI) (Applied Biosystems). Standard samples (10 μg mL^{-1}) of substrates and product metabolites (described above) were prepared in 7:3 MeOH:H_2O. The standard samples were used to optimize parameters for direct injection. Declustering potential (DP), collision exit potential (CXP), collision energy (CE), and entrance potential (EP) were optimized for each analyte. The parameters used were as follows: DP (V), −35, 3; CXP (V), −3, 45; CE (V), −50, 25; EP (V), −10, input temperature of 400 °C.

LC-IT-MS/MS

Experiments were performed on an HPLC (Shimadzu) coupled to an Esquire 6000 IT-MS (Bruker) operating in positive $[M+H]^+$ and negative $[M-H]^-$ ESI mode. The parameters used were as follows: nebulizer, 30 psi; dry gas flow, 8.0 L min^{-1}; dry heater temperature, 325 °C; capillary voltage, 4.5 kV; collision cell energy, 0.5 V in negative mode and 1.0 V in positive mode; smart parameter settings, *m/z* 300 for negative mode and *m/z* 277 for positive mode; full-MS scan range, *m/z* 100–600; and flow (splitter) 0.1 mL min^{-1}. Spectra were obtained in auto MS/MS mode with a CE of 20–40 eV for all *m/z* in the analyzed range. Data Analysis 4.0 software was used for spectral analysis.

LC-SPE-NMR

The LC-SPE-NMR system contained the following instruments: LC system 1200 series, GmbH, G1311A quaternary pump, G1322A degasser, G1315D, photodiode array detector, G1329A autosampler (Agilent, Barueri, SP, Brazil); automatic cartridge exchanger Bruker/Spark Prospekt 2 SPE unit (Bruker BioSpin, Rheinstetten, Germany), containing SPE cartridges (HySphere Resin GP, 10 × 2.0 mm, 10 μm spherical polydivinylbenzene stationary phase); Bruker Daltonik NMR 600 MHz spectrometer with a 14.1 Tesla magnet, $^1H\{^{13}C, ^{15}N\}$ TCI triple resonance cryogenically-cooled probe head. The software used for data acquisition was HYSTAR v. 3.2 (Bruker BioSpin GmbH).

GC-MS

GC experiments were performed in electron impact (EI) ionization mode (70 eV). The split mode was used. An aliquot (1 μL) of the sample was injected onto the GC-MS outfitted with an Optima-5 column (30 × 0.25 mm and film 0.25 μm; Shimadzu) starting at 70 °C. The method used was as follows: 70 °C (6 min), 15 °C min^{-1} up to 160 °C, 5 °C min^{-1} up to 200 °C, 200 °C for 2 min, 20 °C min^{-1} up to 260 °C; 260 °C for 10 min. The flow rate was 1.2 mL min^{-1}. The data were analyzed using GCMS Real-Time Analysis® (Shimadzu) and the National Institute of Standards & Technology (NIST) Mass Spectral Library.

Results

Optimization of conditions for substrate biotransformation

The maximum concentration of substrate with visible *C. gloeosporioides* mycelial growth after 15 days of incubation was 1 mg mL^{-1}. To ensure the biotransformation of substrates, the experiments were subsequently carried out using 100 μg mL^{-1} of the substrate, a concentration that did not visibly cause toxicity to the microorganism. Afterwards, the filtrates of culture media containing mycelia were extracted with EtOAc, and the EtOAc extracts were analyzed for the metabolite profile of each substrate biotransformation.

Biotransformation of zingerone to the zingerone dimer and its isolation

Large-scale biotransformation of zingerone leads to EtOAc extract (B) (960 mg), which, after chromatographic purification, yielded the zingerone dimer (**1**) (4.0 mg). The structure of **1** was elucidated using ^1H

NMR, high-resolution MS (Bruker Daltonics, Micromass TOF–QII-ESI-TOF), and comparison with literature (Slavova-Kazakova et al. 2015). The zingerone dimer (**1**) had a molecular ion *m/z* 409.1648 ($[M+Na]^+$) using positive mode and an *m/z* 385.1700 ($[M-Na]^-$) using the negative mode, indicating the molecular formula $C_{22}H_{26}O_6$ and an M of *m/z* ($C_{22}H_{26}O_6$, 386.1729 calcd.). Direct injection in negative mode showed an $[M-H]^-$ ion at *m/z* 385 and the fragment ions *m/z* 370 and *m/z* 327. The ^{1}H NMR spectrum revealed signals for aromatic hydrogens at δ_H 6.75 (*d*; $J=4.0$ Hz) and δ_H 6.73 (*d*; $J=4.0$ Hz), indicating a *meta* relationship of hydrogens from 2 tetrasubstituted aromatic rings. The symmetry of the molecule generates overlapped signals since some protons are chemically and magnetically equivalent. Likewise, the signal at δ_H 3.92 (*s*, 6H) was attributed to the 2 methoxyl groups bound to the aromatic rings. Another singlet observed at δ_H 2.16 (*s*, 6H) was characteristic of a methyl ketone group. Two triplets at δ_H 2.78 (*t*, 4H) and δ_H 2.88 (*t*, 4H) were attributed to methylene groups, confirming the structure of the zingerone dimer (**1**) (Figure 1).

Metabolite profiling of [6]-gingerol, [6]-gingerol-D3, zingerone-D5 and methyl-[6]-gingerol biotransformation by C. gloeosporioides

The chromatographic analysis of EtOAc extracts revealed complete substrate degradation by day 10, observed by the lack of the [6]-gingerol peak at (t_R) = 21.5 min (Figure 2(A)). The product metabolites were identified as 4-(2-hydroxyethyl)-2-methoxyphenol (**2**) ((t_R) = 12.5 min) and 5,5′-bis(2-hydroxyethyl)-3,3′-dimethoxy-[1,1′-biphenyl]-2,2′-diol (**3**) ((t_R) = 16.3 min).

4-(2-hydroxyethyl)-2-methoxyphenol (**2**) was identified by the $[M-H]^-$ ion at *m/z* 167 and by characteristic signals in the ^{1}H NMR (600 MHz) (Christophoridou and Dais 2009), including δ_H 6.65 (*dd*, $J=8.0$ and 2.0 Hz, 1H), δ_H 6.70 (*d*, $J=8.0$ Hz, 1H), and δ_H 6.79 (*d*, $J=2.0$ Hz, 1H), which are typical of a 1,2,4-trisubstituted aromatic ring. The presence of a methoxyl group and 2 methylene groups are shown by the singlet at δ_H 3.83 (*s*, 3H) and 2 triplets at δ_H 2.73 (*t*, 2H) and δ_H 3.70 (*t*, 2H), respectively.

Compound (**3**) is a biphenol dimer. The structure was confirmed by the $[M-H]^-$ ion at *m/z* 333 with fragment ions *m/z* 287, 215, 187, 171 and 143. In the ^{1}H NMR, the signal at δ_H 3.89 (*s*, 6H) was attributed to the 2 methoxyl groups, and the 2 triplets at δ_H 2.75 (*t*, 4H) and δ_H 2.77 (*t*, 4H) were attributed to methylene groups. The aromatic hydrogens at δ_H 6.75 (*d*; $J=2.0$ Hz, 2H) and δ_H 6.73 (*d*; $J=2.0$ Hz, 2H) indicate the symmetry of this molecule (Pulvirenti et al. 2017).

SRM analysis (*LC-ESI-MS/MS*) was used with transitions of *m/z* 167 to 93 and *m/z* 333 to 215 to evaluate the time course of the biotransformation of [6]-gingerol to compounds **2** and **3** (days 1–7 and 10) (Figure 2(B)). Results were compared to controls (A and B). The 4-(2-hydroxyethyl)-2-methoxyphenol (**2**) peak was higher in intensity on days 1 and 5, but the biphenol dimer (**3**) was highest on day 10.

To investigate the possible reactions involved in the biotransformation of [6]-gingerol, and to eliminate the possibility that compound **2** was a derivative of tyrosol or another fungal metabolite (Bungihan et al. 2013), we carried out the biotransformation of deuterated [6]-gingerol ([6]-gingerol-D_3; 54%), administering the labelled compound as a substrate in fungal culture.

We also used penta-deuterated zingerone (zingerone-D_5; 66.3%) (100 μg mL^{-1}) as a model compound in biotransformation reactions with *C. gloeosporioides*. The time course of the biotransformation was monitored by analyzing EtOAc extracts from days 1, 3, 6, 8 and 10. The chromatogram (*Method I*) of the EtOAc extracts showed zingerone degradation on day 6 and

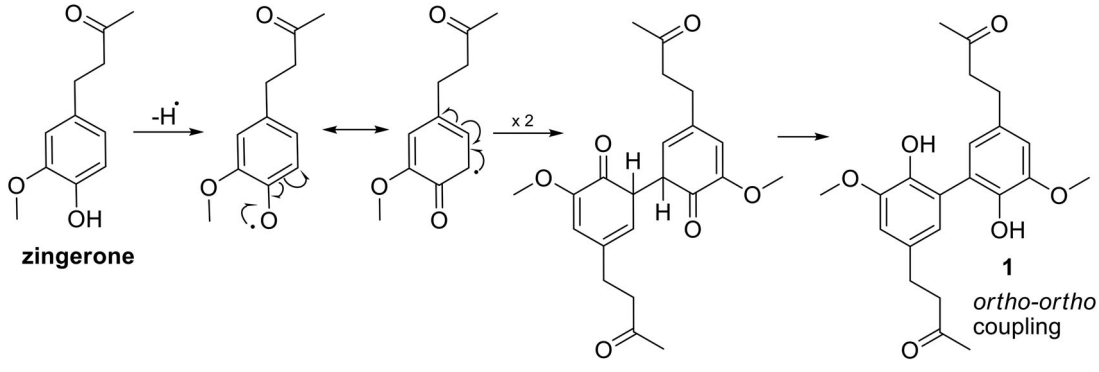

Figure 1. Zingerone dimer (**1**), the product of the biotransformation of zingerone by *C. gloeosporioides*. Phenolic oxidative couplings of zingerone are proposed based on a hydrogen-abstraction of phenol. The zingerone dimer is the product of *ortho–ortho* coupling by enolization, which restores aromaticity to rings.

an increase of zingerone dimer (**1**) (Figure S5, Supplementary Information).

The zingerone biotransformation metabolite profile was also analyzed by LC-MS (*Method III*, LC-IT-MS/MS). Figure 3 shows the ion chromatograms of the EtOAc extract for the time course experiment. Biphenol formation was observed ($[M-H]^-$ ion with *m/z* 385). Fragmentation of the product metabolite (day 10,

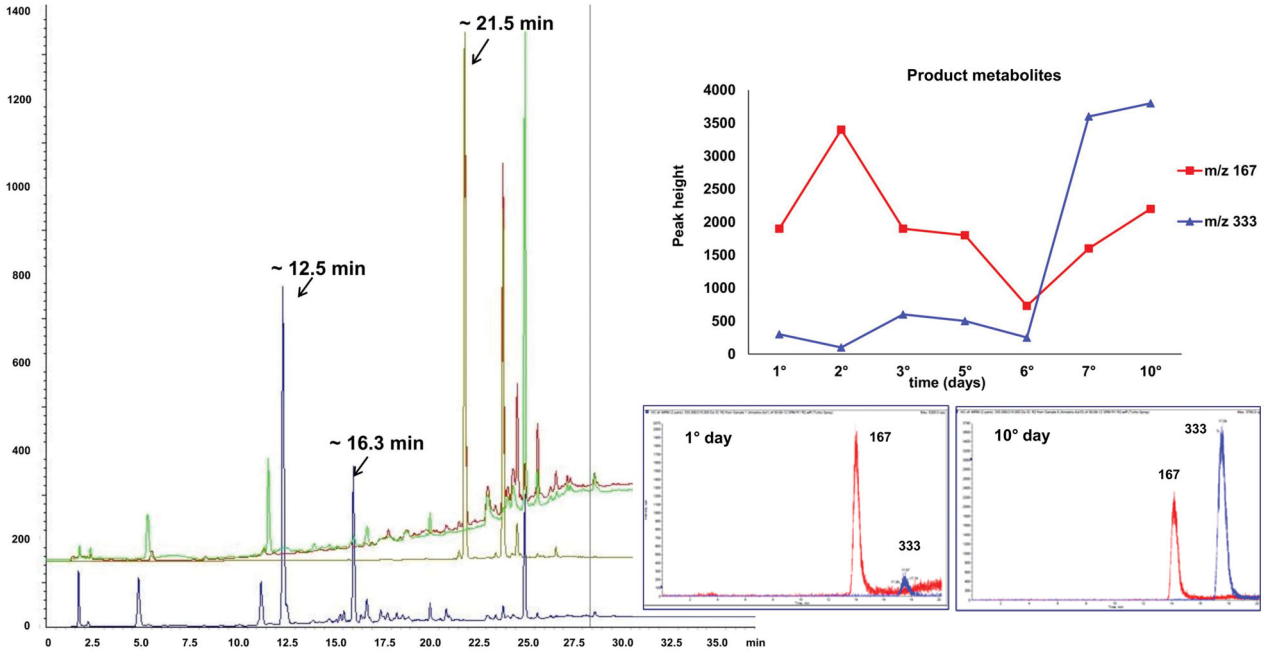

Figure 2. (A) HPLC chromatogram of EtOAc extract of the bioconversion of [6]-gingerol (100 μg mL^{-1}) by *C. gloeosporioides* after 10 days. Control (A): without substrate addition; Control (B): substrate without fungal inoculation ((t_R) = 21.5 min). EtOAc extract: consumption of [6]-gingerol by the fungus shows a lack of the substrate peak at (t_R) = 21.5 min. HPLC conditions: *Method II* with water (A):MeOH (B); (B) SRM analysis (LC-ESI-MS/MS) with transitions of *m/z* 167 to 93 and *m/z* 333 to 215, product metabolites (**2**) and (**3**), respectively, during time course of biotransformation (days 1–7 and 10).

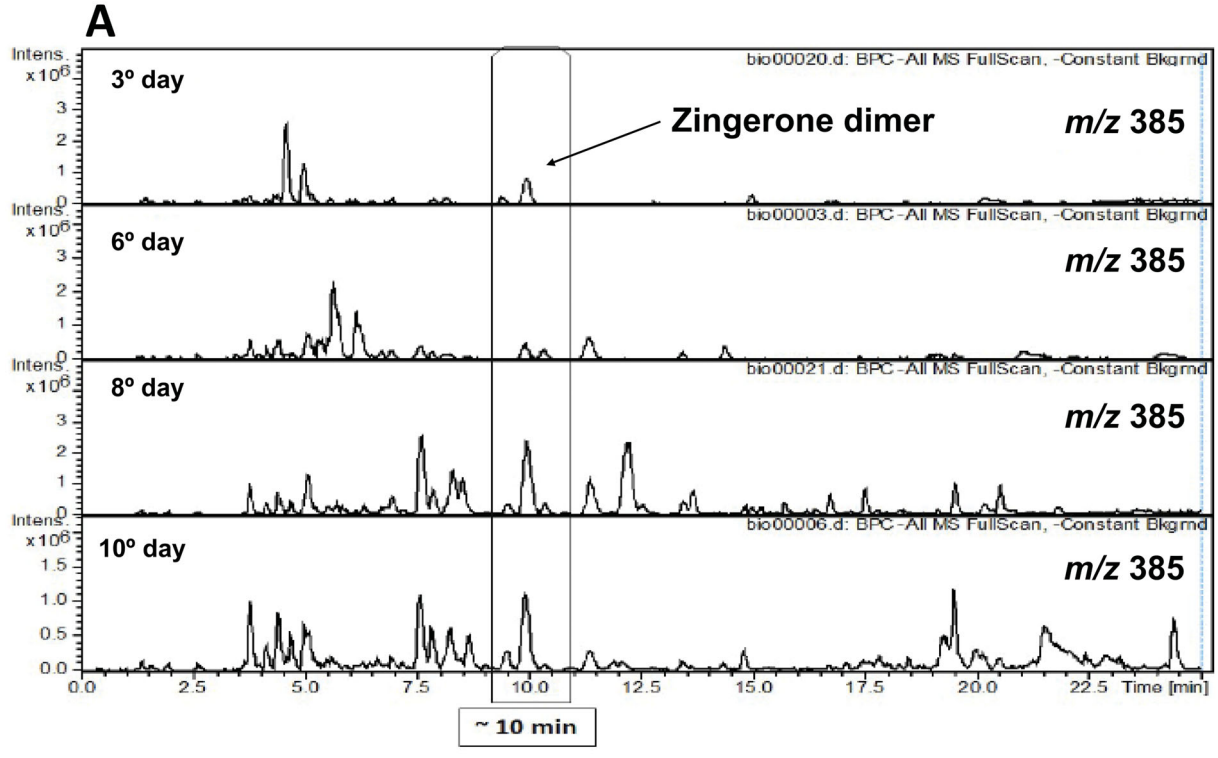

Figure 3. Representative LC-MS extracted ion chromatogram for EtOAc extract obtained from culture medium of *C. gloeosporioides* with 100 μg mL^{-1} of zingerone and its metabolites. *Method III* was used for the experiment (LC-IT-MS/MS).

peak at (t_R) = 10.0 min) produced the fragment ions *m/z* 370.03 and 327.01, characteristic of compound **1**.

The bioconversion of zingerone-D_5 led to distinct deuterium labelling. The $[M-H]^-$ ion at *m/z* 389.12, corresponding to the penta-deuterated zingerone dimer, confirmed that zingerone was recognized by *C. gloeosporioides* enzymes and was incorporated into its metabolic pathways (Figure S9, Supplementary Information).

After confirmation that labelled zingerone was transformed by *C. gloeosporioides* into the labelled dimer, we performed large-scale biotransformations of [6]-gingerol and [6]-gingerol-D_3 for 10 days, which afforded 15.0 mg of EtOAc extract.

The transformation of the carbon chain of [6]-gingerol-D_3 was verified by identification of the biphenol dimer-D_3 in the EtOAc extract using LC-IT-MS/MS (*Method III*). Based on the fragmentation pattern (Figure S14, Supplementary Information), it is possible that the biotransformation of [6]-gingerol could occur by a fungal enzyme-catalyzed Baeyer–Villiger reaction followed by hydrolysis, affording 4-(2-hydroxyethyl)-2-methoxyphenol (**2**) (Figure 4).

Methyl-[6]-gingerol, a metabolite from the ginger root (Li et al. 2009), was obtained by chemical derivatization of [6]-gingerol, and the derivative was supplied to *C. gloeosporioides* cultures with the same optimized conditions. The EtOAc extract obtained on day 5 was analyzed using *Method II* (water (A):MeOH (B)), GC-MS and LC-IT-MS/MS (*Method III*) (Figures S19–S25 and Table S1, Supplementary Information). The metabolic products 3-methoxy-4-hydroxyphenylethanol (**2**) and 3,4-dimethoxyphenylethanol (**4**) were observed. The production of compound **2** could be related to a remote possibility that some [6]-gingerol remained after purification of methyl-[6]-gingerol, or that a demethylation reaction occurred. Compound **4** was assigned based on the GC-MS observation of the *m/z* 182 ion and its fragments (*m/z* 151, 135, 107, 91, 77, and 51), as well as ^{1}H NMR data and a comparison with literature (Shahane et al. 2008). This indicates methyl-[6]-gingerol follows the same fungal degradation pathway as [6]-gingerol (Figure 4).

The chromatogram peaks observed between (t_R) = 5 and 7 min, which were absent in control (B), were analyzed in positive mode ((+)-ESI-MS/MS). The $[M+H]^+$ ions *m/z* 325 and 327 and the fragment ions (*m/z* 307, 289, 191, and 133; *m/z* 309, 291, 273, 221, 191, 177, and 151, respectively) suggested the product metabolites **M1** (*m/z* 325), **M2** (*m/z* 327), and **M3** (*m/z* 327), products of hydroxylation and reduction reactions. Compound **M1** eluted at (t_R) = 6.4 min. **M2** and **M3** were identified in peaks with different retention times: (t_R) = 6.0 and 6.3 min and (t_R) = 5.8 and

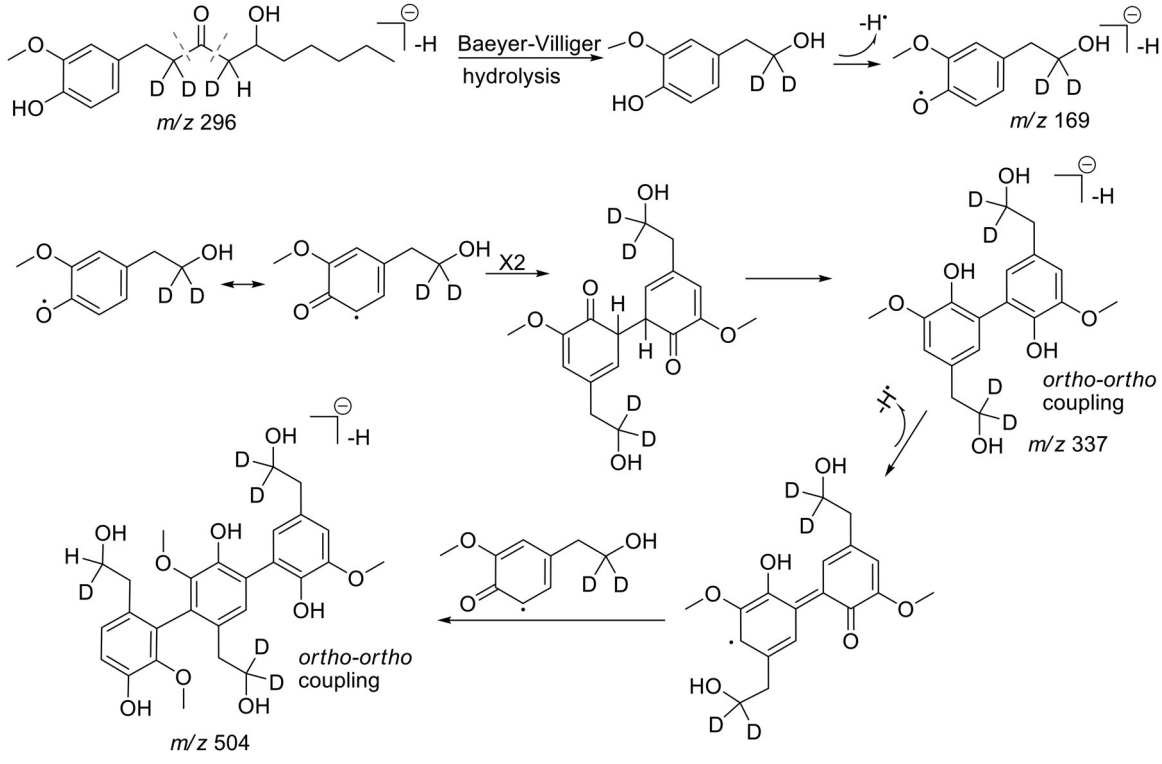

Figure 4. Proposed fungal degradation pathway of [6]-gingerol-D_3. The $[M-H]^-$ with *m/z* 503 indicated a phenol trimer-D_3 product of phenolic oxidative coupling of 4-(2-hydroxyethyl)-2-methoxyphenol (**2**); the ions at *m/z* 169 and *m/z* 337 are related to the deuterated product metabolites (**2**) and (**3**) (Figure 2(B), *m/z* 167 and *m/z* 333, respectively).

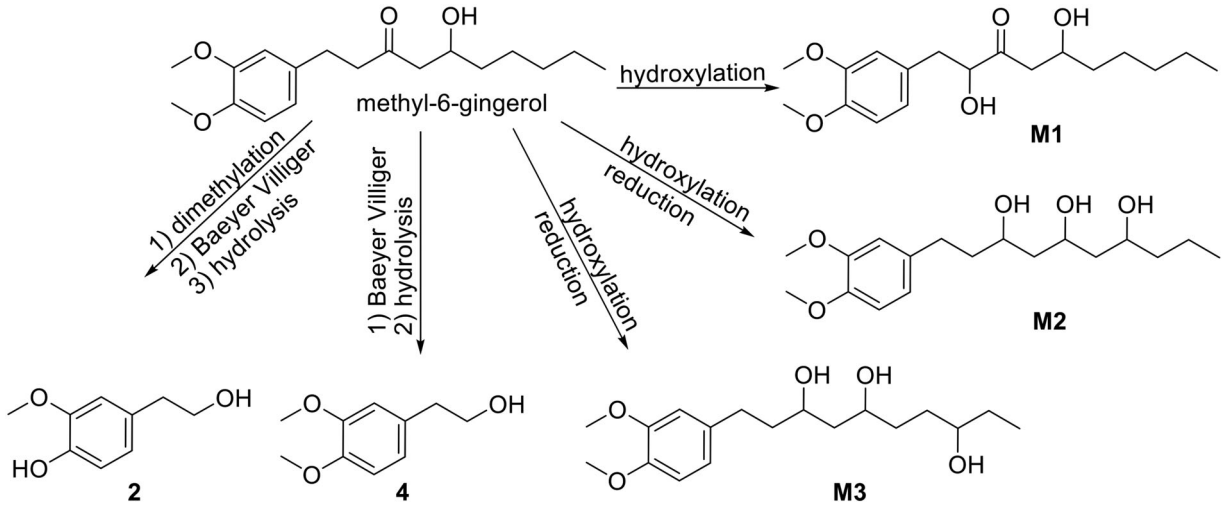

Figure 5. Metabolic products of the bioconversion of methyl-[6]-gingerol.

5.9 min, respectively, which indicates that both may exist as diastereoisomer pairs (Figure 5).

Metabolite profiling of [6]-shogaol biotransformation by C. gloeosporioides

The day 5 EtOAc extract obtained after [6]-shogaol incubation with the fungus revealed substrate consumption by *C. gloeosporioides*, although higher product metabolite intensities were observed after 10 days. Five compounds were identified by MS as product metabolites from [6]-shogaol biodegradation: 3-methoxy-4-hydroxyphenylethanol (**2**), 2-octenoic acid, 2-(4-hydroxy-3-methoxyphenyl)ethyl ester (**5**), [6]-gingerdiol (**6**), tyrosol (**7**), and octanoic acid, 2-(4-hydroxy-3-methoxyphenyl)ethyl ester (**8**).

GC-MS analysis of the day 5 EtOAc extract allowed the identification of compounds **2**, **5**, **6**, and **7**, which were confirmed by comparing to literature data (Kikuzaki et al. 1992; Jolad et al. 2004; Christophoridou and Dais 2009). Compounds **6** and **8** were also found on day 10. The characteristic ions *m/z* 168, 137 and 122 belong to 4-(2-hydroxyethyl)-2-methoxyphenol (**2**), which was also identified as the product metabolite from [6]-gingerol and methyl-[6]-gingerol biodegradation, as previously discussed. The *m/z* 292 ion, together with the *m/z* 137 base peak, was suggestive of the ester **5**, an intermediate metabolite in a Baeyer–Villiger reaction. The Baeyer–Villiger reaction could be catalyzed by an oxidase enzyme, such as a peroxidase or a laccase (Figure 6), reinforcing our previous proposed reaction pathway for 4-(2-hydroxyethyl)-2-methoxyphenol (**2**) (Figure 4).

The identification of molecular and fragmentation ions *m/z* 296, 278, 260, 207, 189, 175, 163, 150 and 137 suggested the presence of [6]-gingerdiol (**6**), a natural constituent of *Zingiber officinale* roots (Kikuzaki et al. 1992; Jolad et al. 2004). [6]-gingerdiol (**6**) could be a product of [6]-shogaol carbonyl reduction, a reaction which has been observed in *C. gloeosporioides* cultures with several other substrates (García-Pajón et al. 2003). Additionally, in a previous study of *Aspergillus niger* cultures supplemented with [6]-shogaol, product metabolites were mostly formed through double bond and ketone reduction, and hydroxylation (Jo et al. 2016).

The parent peak ion at *m/z* 294 with a base peak *m/z* 137 could be hydroxylation of [6]-shogaol to give [6]-gingerol, as fragment data match the literature values. However, the retention time observed for compound **8** ($(t_R) = 28.5$ min) was quite different from the standard [6]-gingerol ($(t_R) = 27.8$ min, Figure S27) using the same experimental conditions. In addition, the product ions expected from the thermal degradation of [6]-gingerol were absent in the GC-MS chromatogram. Thus, the *m/z* 294 ion was attributed to the formation of ester **8**, which could be the product of the double bond reduction of ester **5** (Gan et al. 2016). Tyrosol (**7**), a molecule previously isolated from *C. gloeosporioides* (Bungihan et al. 2013), was identified by the ion with *m/z* 138 and a base peak at *m/z* 107 (Figure 7).

The metabolite profile of [6]-shogaol biotransformation was also analysed by LC-MS (*Method III*, LC-IT-MS/MS) on days 5 and 10 (Figure 8). Product metabolites were identified, especially with retention times between 5 and 10 minutes, that were not observed in the control samples.

The $[M-H]^-$ ion at *m/z* 295 ($(t_R) = 7.2$ min) with a fragment ion at *m/z* 280 is related to [6]-gingerdiol (**6**)

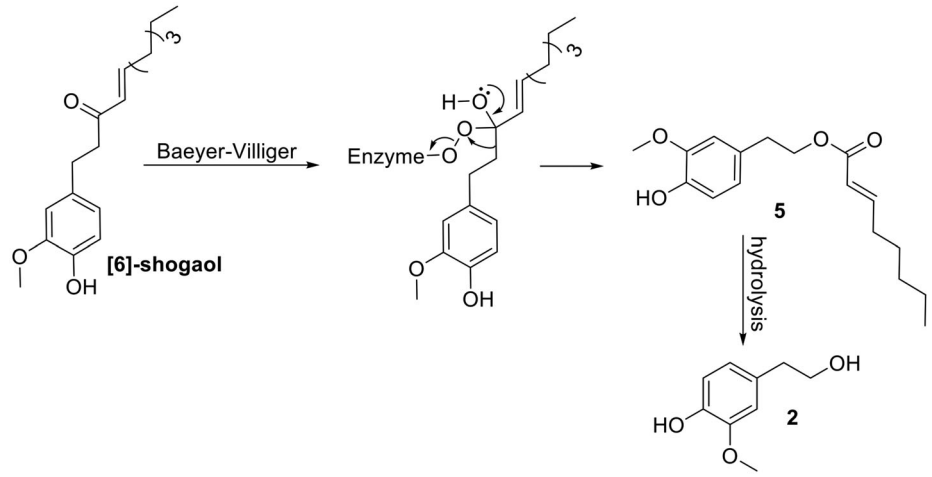

Figure 6. Proposed degradation pathway of [6]-shogaol by *C. gloeosporioides*. The ester (**5**) is a possible intermediate metabolite in a Baeyer–Villiger reaction, leading to the formation of 4-(2-hydroxyethyl)-2-methoxyphenol (**2**).

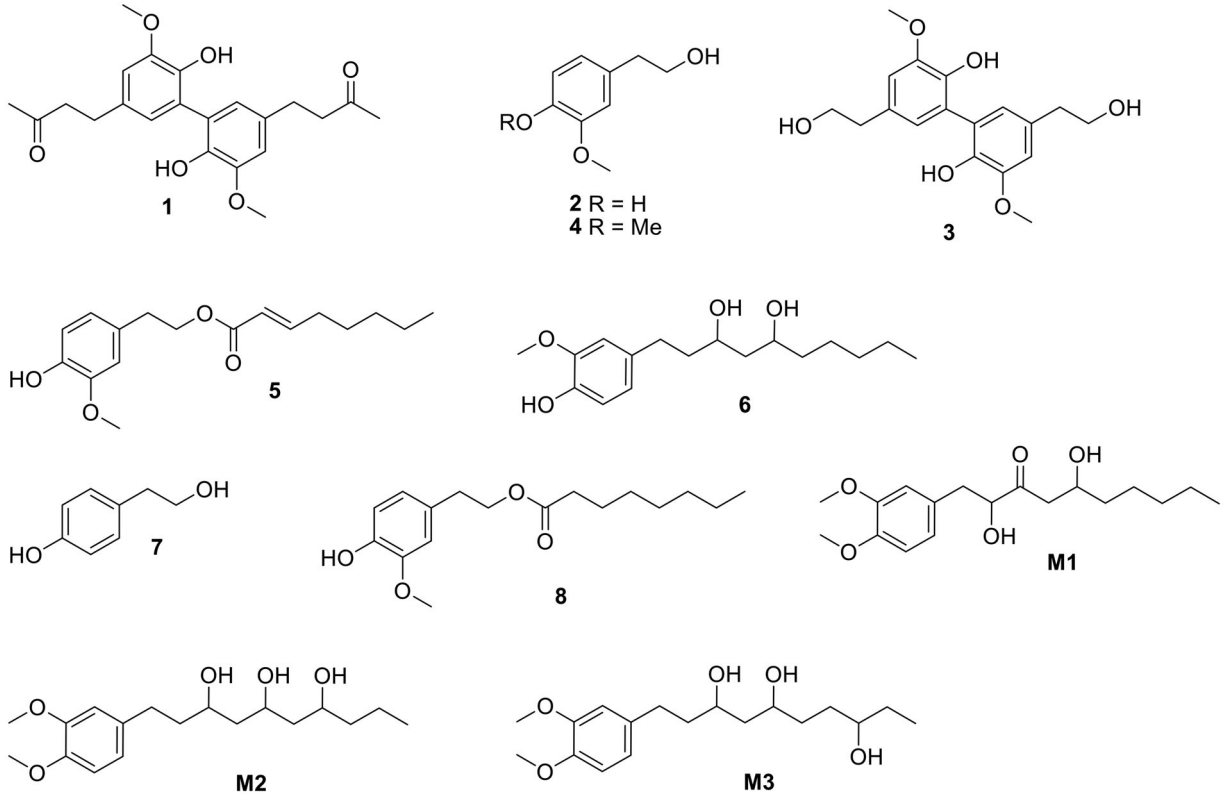

Figure 7. Metabolic products from the biotransformation of ginger constituents (zingerone, [6]-shogaol, [6]-gingerol, and methyl-[6]-gingerol) by *C. gloeosporioides*.

(Tao et al. 2009), and the $[M-H]^-$ ion at *m/z* 291((t_R) = 9.3 min) with fragments at *m/z* 276, 156 and 123 is related to the proposed ester **5**. Compounds **5** and **6** were identified in both day 5 and day 10 extracts. The $[M-H]^-$ ion at *m/z* 291 could also be [6]-gingerdione, a product of oxidoreductase activity. However, the fragment ions in the spectra were not identical to fragment ions from confirmed [6]-gingerdione using the same conditions (ESI-MS/MS) (Tao et al. 2009).

Discussion

Many members of the *Colletotrichum* genus are plant pathogens. Species of this genus have been widely investigated in order to understand how their metabolic cause crop diseases (García-Pajón et al. 2003). However, the biotransformation of ginger metabolites by *C. gloeosporioides* has not been previously investigated.

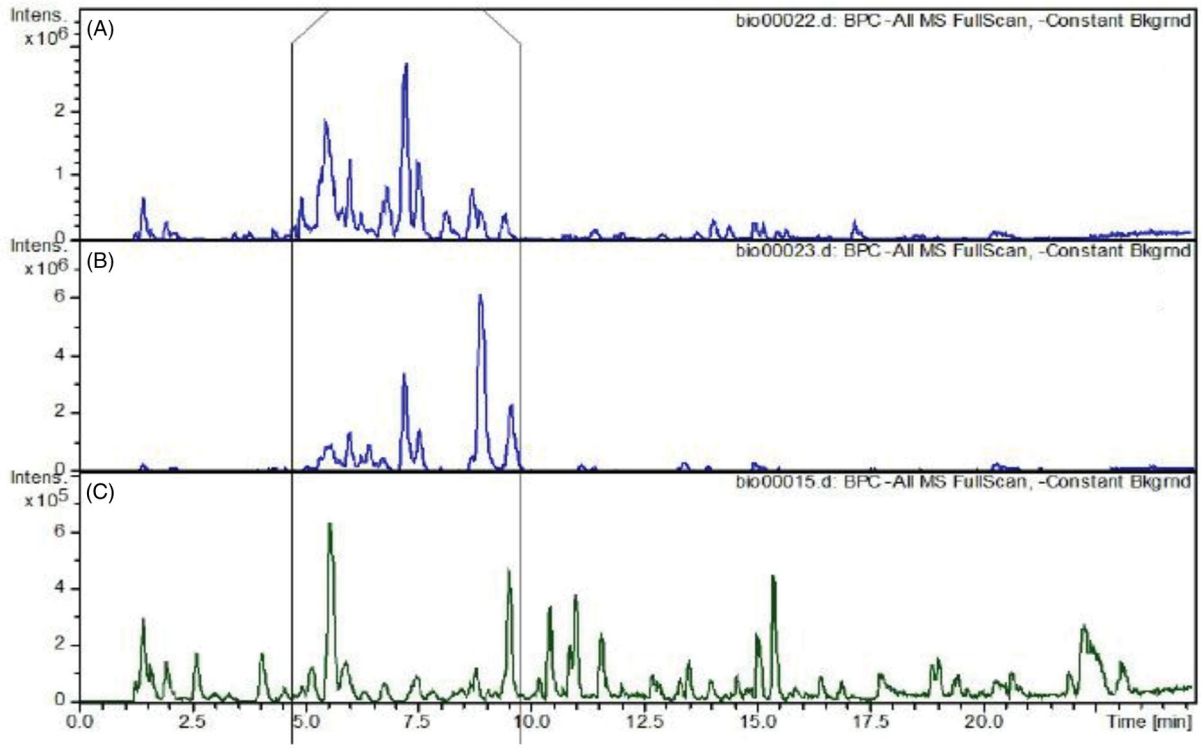

Figure 8. Chromatogram of EtOAc after 5 and 10 days of [6]-shogaol (100 μg mL^{-1}) biodegradation by *C. gloeosporioides*. (A) EtOAc extract analysis after 5 days; (B) EtOAc extract analysis after 10 days; (C) same as (B) but without *C. gloeosporioides*; HPLC conditions: *Method III*, using water (A):ACN (B) with 0.1% *v/v* formic acid in both solvents (LC-IT-MS/MS, Full scan in negative mode).

The fungal biotransformation of substrates from ginger (zingerone, [6]-shogaol, [6]-gingerol, and methyl-[6]-gingerol) afforded 11 metabolic products of fungal bioconversion (Figure 7). Zingerone and [6]-gingerol were transformed into the zingerone dimer (**1**) and 5,5′-bis(2-hydroxyethyl)-3,3′-dimethoxy-[1,1′-biphenyl]-2,2′-diol (**3**), respectively. Biphenols are useful compounds for organic synthesis and have many industrial, pharmaceutical, and agricultural applications (Bonrath et al. 2007; Engelmann et al. 2015). The zingerone dimer was synthesized previously and was demonstrated to be a biphenol with antioxidant activity (Marchiani et al. 2013; Slavova-Kazakova et al. 2015). The biphenol dimer (**3**) reduces the catalytic activity of yeast α-glucosidase, an enzyme related to diabetic diseases (Pulvirenti et al. 2017).

Oxidase enzymes (peroxidases and laccases) likely formed the zingerone dimer by phenolic oxidative coupling of the products of free radical reactions (Jeon et al. 2012). Biphenols with C–C couplings are mostly produced by fungal laccase enzymes, which are copper-containing oxidoreductases with redox potential and have applications in biotechnology (Hollmann et al. 2011; Jeon et al. 2012; Abdel-Mohsen et al. 2014; Engelmann et al. 2015). Previously, a laccase from *Colletotrichum lagenarium* was shown to degrade dyes in industrial effluents (Wang et al. 2016). A laccase from *C. gloeosporioides* also metabolises epicatechin from avocado (Guetsky et al. 2005). The biphenol dimer (**3**) could be also a product of phenolic oxidative coupling catalyzed by oxidase enzymes (Figure 4), probably initiated by the hydrogen-abstraction of compound **2**, which is a product metabolite identified from [6]-gingerol biodegradation (Jeon et al. 2012).

Compound **2** was obtained when supplying methyl-[6]-gingerol and [6]-shogaol as substrates for *C. gloeosporioides*. Another intermediate of the proposed reaction pathway for [6]-shogaol biodegradation was the ester (**5**) (Figure 6), the presence of which suggests a fungal enzyme-catalysed Baeyer–Villiger reaction, followed by hydrolysis.

Conclusions

In conclusion, labelling the pungent constituents of ginger with deuterium allowed verification of the fungal biotransformation of the metabolites by GC-MS, LC-MS/MS, and LC-SPE-NMR. The bioconversion of [6]-gingerol and zingerone led to biphenol dimers, suggesting that *C. gloeosporioides* metabolises these substrates using an oxidase enzyme, possibly a laccase.

For the 4-(2-hydroxyethyl)-2-methoxyphenol metabolite was proposed a degradation pathway by *C. gloeosporioides* involving Baeyer–Villiger reaction and subsequent hydrolysis. *Colletotrichum gloeosporioides* enzymes mostly performed reduction and hydroxylation reactions on methyl-[6]-gingerol and [6]-shogaol. We report for the first time the ability of *C. gloeosporioides* to perform phenolic oxidative coupling reactions. Our results demonstrate the utility of fungi in transforming complex metabolites into biphenols, which have broad industrial interest.

Disclosure statement

No potential conflict of interest was reported by the author(s).

Funding

The present work was financially supported by the São Paulo Research Foundation (FAPESP) (Grant # 14/50249-8) and the Coordination for the Improvement of Higher Education Personnel (CAPES, Finance Code 001).

ORCID

Leonardo Toffano http://orcid.org/0000-0002-7591-0530
João Batista Fernandes http://orcid.org/0000-0002-2924-3327
Maria Fátima das Graças Fernandes da Silva http://orcid.org/0000-0002-7081-817X
Lorena Ramos Freitas de Sousa http://orcid.org/0000-0002-2506-8365
Paulo Cezar Vieira http://orcid.org/0000-0003-4207-6217

References

Abdel-Mohsen HT, Conrad J, Beifuss U. 2014. Laccase-catalyzed synthesis of catechol thioethers by reaction of catechols with thiols using air as an oxidant. Green Chem. 16(1):90–95.

Ahmad B, Rehman MU, Amin I, Arif A, Rasool S, Bhat SA, Afzal I, Hussain I, Sheikh B, Mir MR. 2015. A review on pharmacological properties of zingerone (4-(4-Hydroxy-3-methoxyphenyl)-2-butanone). Sci World J. 2015:816364.

Azimi P, Ghiasvand R, Feizi A, Hosseinzadeh J, Bahreynian M, Hariri M, Khosravi-Boroujeni H. 2016. Effect of cinnamon, cardamom, saffron and ginger consumption on blood pressure and a marker of endothelial function in patients with type 2 diabetes mellitus: A randomized controlled clinical trial. Blood Press. 25(3):133–140.

Baliga MS, Shivashankara AR, Haniadka R, Palatty PL, Arora R, Fayad R. 2013. Bioactive food as dietary interventions for liver and gastrointestinal disease. vol. 11. Cambridge (MA): Academic Press; p. 187–199.

Bartels EM, Folmer VN, Bliddal H, Altman RD, Juhl C, Tarp S, Zhang W, Christensen R. 2015. Efficacy and safety of ginger in osteoarthritis patients: A meta-analysis of randomized placebo-controlled trials. Osteoarthritis Cartil. 23(1):13–21.

Bhattarai S, Tran VH, Duke CCJ. 2007. Stability of [6]-gingerol and [6]-shogaol in simulated gastric and intestinal fluids. J Pharm Biomed Anal. 45(4):648–653.

Bonrath W, Eggersdorfer M, Netscher T. 2007. Catalysis in the industrial preparation of vitamins and nutraceuticals. Catal Today. 121(1–2):45–57.

Bungihan ME, Tan MA, Takayama H, Dela Cruz TEE, Nonato MG. 2013. A new macrolide isolated from the endophytic fungus *Colletotrichum* sp. Philippine Sci Lett. 6:57–73.

Choi JG, Kim SY, Jeong M, Oh MS. 2018. Pharmacotherapeutic potential of ginger and its compounds in age-related neurological disorders. Pharmacol Ther. 182:56–69.

Choi JW, Park HY, Oh MS, Yoo HH, Lee SH, Ha SK. 2017. Neuroprotective effect of [6]-paradol enriched ginger extract by fermentation using Schizosaccharomyces pombe. J Funct Foods. 31:304–310.

Christophoridou S, Dais P. 2009. Detection and quantification of phenolic compounds in olive oil by high resolution ^{1}H nuclear magnetic resonance spectroscopy. Anal Chim Acta. 633(2):283–292.

Citronberg J, Bostick R, Ahearn T, Turgeon DK, Mack TR, Djuric Z, Ananda S, Brenner DE, Zick SM. 2013. Effects of ginger supplementation on cell-cycle biomarkers in the normal-appearing colonic mucosa of patients at increased risk for colorectal cancer: Results from a pilot, randomized, and controlled trial. Cancer Prev Res. 6(4):271–281.

Da Silva JA, Becceneri AB, Mutti HS, Martin ACBM, Silva M, Fernandes JB, Vieira PC, Cominetti MR. 2012. Purification and differential biological effects of ginger-derived substances on normal and tumor cell lines. J Chromatogr B. 903:157–162.

Engelmann C, Illner S, Kragl U. 2015. Laccase initiated C–C couplings: Various techniques for reaction monitoring. Process Biochem. 50(10):1591–1599.

Fuzer AM, Martin ACBM, Becceneri AB, da Silva JÁ, Vieira PC, Cominetti MR. 2019. [10]-Gingerol affects multiple metastatic processes and induces apoptosis in MDAMB- 231 Breast Tumor Cells. Anticancer Agents Med Chem. 19(5): 645–654.

Gan Z, Liang Z, Chen X, Wen X, Wang Y, Li M, Ni Y. 2016. Separation and preparation of 6-gingerol from molecular distillation residue of Yunnan ginger rhizomes by high-speed counter-current chromatography and the antioxidant activity of ginger oils in vitro. J Chromatogr B Analyt Technol Biomed Life Sci. 1011:99–107.

García-Pajón CM, Hernández-Galán R, Collado IG. 2003. Biotransformations by *Colletotrichum* species. Tetrahedron: Asymmetry. 14(10):1229–1239.

Guetsky R, Kobiler I, Wang X, Perlman N, Gollop N, Avila-Quezada G, Hadar I, Prusky D. 2005. Metabolism of the flavonoid epicatechin by laccase of *Colletotrichum gloeosporioides* and its effect on pathogenicity on avocado fruits. Phytopathology. 95(11):1341–1348.

Ho S, Chang K, Lin C. 2013. Anti-neuroinflammatory capacity of fresh ginger is attributed mainly to 10-gingerol. Food Chem. 141(3):3183–3191.

Hollmann F, Arends I, Buehler K, Schallmey A, Buhler B. 2011. Enzyme-mediated oxidations for the chemist. Green Chem. 13(2):226–265.

Jeon JR, Baldrian P, Murugesan K, Chang YS. 2012. Laccase-catalysed oxidations of naturally occurring phenols: From *in vivo* biosynthetic pathways to green synthetic applications. Microb Biotechnol. 5(3):318–332.

Jo SK, Kim IS, Rehman SU, Ha SK, Park HY, Park YK, Yoo HH. 2016. Characterization of metabolites produced from the biotransformation of [6]-shogaol formed by *Aspergillus niger*. Eur Food Res Technol. 242(1):137–142.

Jolad SD, Lantz RC, Solyom AM, Chen GJ, Bates RB, Timmermann BN. 2004. Fresh organically grown ginger (*Zingiber officinale*): Composition and effects on LPS-induced PGE2 production. Phytochemistry. 65(13): 1937–1954.

Kikuzaki H, Tsai SM, Nakatani N. 1992. Gingerdiol related compounds from the rhizomes of *Zingiber officinale*. Phytochemistry. 31(5):1783–1786.

Kou X, Wang X, Ji R, Liu L, Qiao Y, Lou Z, Ma C, Li S, Wang H, Ho C-T. 2018. Ocurrence, biological activity and metabolism of [6]-shogaol. Food Funct. 9(3):1310–1327.

Kubra IR, Rao LJM. 2012. An impression on current developments in the technology, chemistry, and biological activities of ginger (*Zingiber officinale* Roscoe). Crit Rev Food Sci Nutr. 52(8):651–688.

Kumar NV, Murthy PS, Manjunatha JR, Bettadaiah BK. 2014. Synthesis and quorum sensing inhibitory activity of key phenolic compounds of ginger and their derivatives. Food Chem. 159:451–457.

Lee SS. 1995. Re-examination of [6]-shogaol biotransformation by *Aspergillus niger*. Arch Pharm Res. 18(2):136–137.

Lee SS, Lee WY. 1995. Biotransformation of dehydroparadols by *Aspergillus niger*. Arch Pharm Res. 18(6):458–461.

Li X, Ziyang L, Zhang H, Zhao L, Wu H, Zhang G, Wu Y, Chai Y. 2009. Rapid LC-TOFMS separation and identification of diarylheptanoids and gingerol-related compounds in dried ginger. Chroma. 69(5–6):531–536.

Marchiani A, Mammi S, Siligardi G, Hussain R, Tessari I, Bubacco L, Delogu G, Fabbri D, Dettori MA, Sanna D, et al. 2013. Small molecules interacting with α-synuclein: Antiaggregating and cytoprotective properties. Amino Acids. 45(2):327–338.,

Martin ACBM, Fuzer AM, Becceneri AB, da Silva JÁ, Tomasin R, Denoyer D, Kim SH, McIntyre KA, Pearson HB, Yeo B, et al. 2017. [10]-gingerol induces apoptosis and inhibits metastatic dissemination of triple negative breast cancer in vivo. Ocontarget. 8(42):72260–72271.

Mashhadi NS, Ghiasvand R, Askari G, Hariri M, Darvishi L, Mofid MR. 2013. Anti-oxidative and anti-inflammatory effects of ginger in health and physical activity: Review of current evidence. Int J Prev Med. 4(1):S36–S42.

Miyazawa M, Nankai H, Kameoka H. 1995. Biotransformations of acyclic terpenoids, (±)-cis-nerolidol and nerylacetone, by plant pathogenic fungus, *Glomerella cingulate*. Phytochemistry. 40(4):1133–1137.

Miyazawa Y, Wada T. 2000. Biotransformation of gamma-terpinene and (−)-alpha-phellandrene by the larvae of common cutworm (*Spodoptera litura*). J Agric Food Chem. 48(7):2893–2895.

Nile SH, Park SW. 2015. Chromatographic analysis, antioxidant, anti-inflammatory, and xanthine oxidase inhibitory activities of ginger extracts and its reference compounds. Industr Crops Prod. 70:238–244.

Prasad S, Tyagi AK. 2015. Ginger and its constituents: Role in prevention and treatment of gastrointestinal cancer. Gastroenterol Res Pract. 2015:142979.

Pulvirenti L, Muccilli V, Cardullo N, Spatafora C, Tringali C. 2017. Chemoenzymatic synthesis and α-glucosidase inhibitory activity of dimeric neolignans inspired by magnolol. J Nat Prod. 80(5):1648–1657.

Semwal RB, Semwal DK, Combrinck S, Viljoen AM. 2015. Gingerols and shogaols: Important nutraceutical principles from ginger. Phytochemistry. 117:554–568.

Shahane S, Louafi F, Moreau J, Hurvois JP, Renaud JL, de Weghe PV, Roisnel T. 2008. Synthesis of alkaloids of *Galipea officinalis* by alkylation of an α-amino nitrile. Eur J Org Chem. 2008(27):4622–4631.

Slavova-Kazakova AK, Angelova SE, Veprintsev TL, Denev P, Fabbri D, Dettori MA, Kratchanova M, Naumov VV, Trofimov AV, Vasil'ev RF, et al. 2015. Antioxidant potential of curcumin-related compounds studied by chemiluminescence kinetics, chain-breaking efficiencies, scavenging activity (ORAC) and DFT calculations. Beilstein J Org Chem. 11:1398–3411.

Stoner GD. 2013. Ginger: Is it ready for prime time? Cancer Prev Res. 6(4):257–262.

Takahashi H, Hashimoto T, Noma Y, Asakawa Y. 1993. Biotransformation of [6]-gingerol and [6]-shogaol by *Aspergillus niger*. Phytochemisty. 34(6):1497–1500.

Tamogami S, Agrawal GK, Rakwal R. 2016. Methyl jasmonate elicits the biotransformation of geraniol stored as its glucose conjugate into methyl geranate in *Achyranthes bidentata plant*. Plant Physiol Biochem. 109:166–170.

Tao Y, Li W, Liang W, Breemen RBV. 2009. Identification and quantification of gingerols and related compounds in ginger dietary supplements using high-performance liquid chromatography-tandem mass spectrometry. J Agric Food Chem. 57(21):10014–10021.

Villalvilla A, da Silva JA, da Largo R, Gualillo O, Vieira PC, Herrero-Beaumont G, Gómez R. 2014. 6-Shogaol inhibits chondrocytes' innate immune responses and cathepsin-K activity. Mol Nutr Food Res. 58(2):256–266. [

Wang B, Yan Y, Tian Y, Zhao W, Li Z, Gao J, Peng R, Yao Q. 2016. Heterologous expression and characterisation of a laccase from *Colletotrichum lagenarium* and decolourisation of different synthetic dyes. World J Microbiol Biotechnol. 32:1–9.